Bursa Uludağ University Journal of The Faculty of Engineering, Vol. 27, No. 1, 2022 RESEARCH

DOI: 10.17482/uumfd.1009101

FOLDED ANGLE DEPENDENT MODAL ANALYSIS OF THE FLAT AND FOLDED PLATES

Can GONENLI *

Received: 13.10.2021 ; revised: 22.03.2022 ; accepted: 23.03.2022

Abstract: The effect of folded angle and boundary condition differences on the natural frequency, which is one of the dynamic characteristics of isotropic thin plates, is investigated. Modal analyzes of flat and folded structures are performed with ANSYS under cantilever and two-side-fixed boundary conditions. The validation of the free vibration results of the structures is performed with Solidworks. The first five natural frequencies of each structure are obtained, and the values in terms of non-dimensional natural frequency parameters are interpreted with the tables and graphics. While both an increase and a decrease can be observed depending on the increase in the folded angle in the first five natural frequencies for the cantilever boundary condition, the effect of the increase in the folded angle on the natural frequencies in the two-sided-fixed structures is much less in the higher folded angle values. It is seen that the reason for the sudden changes in the folded angle - non-dimensional natural frequency graphs is the mode shape change.

Keywords: Folded angle, Free vibration analysis, Finite element method, Thin plate, Modal analysis

Düz ve Bükümlü Plakaların Büküm Açısına Bağlı Modal Analizi

Özet: İzotropik ince plakaların dinamik özelliklerinden biri olan doğal frekans üzerinde bükümlü açı ve sınır koşulu farklılıklarının etkisi araştırılmıştır. Düz ve bükümlü yapıların modal analizleri tek ve çift tarafı sabit sınır koşulları altında ANSYS ile yapılmıştır. Yapıların serbest titreşim sonuçlarının validasyonu Solidworks ile yapılmıştır. Her yapının ilk beş doğal frekansı elde edilmiş ve boyutsuz doğal frekans parametreleri cinsinden değerler tablo ve grafiklerle yorumlanmıştır. Tek tarafı sabit sınır koşulu için ilk beş doğal frekansta büküm açısındaki artışa bağlı olarak hem bir artış hem de bir azalma gözlemlenebilirken, çift taraflı sabit durumda büküm açısındaki artışın doğal frekanslar üzerindeki etkisi yüksek katlanmış açı değerlerinde çok daha azdır. Büküm açısı - boyutsuz doğal frekans grafiklerindeki ani değişimlerin sebebinin mode şekli değişimi olduğu görülmektedir.

Anahtar Kelimeler: Büküm açısı, Serbest titreşim analizi, Sonlu elemanlar yöntemi, İnce plaka, Modal analiz

1. INTRODUCTION

Thin plates are frequently used as a fundamental component in engineering structures. According to the usage areas, thin plates are produced in different geometries and mounted under different boundary conditions. Since such structures operate under different load conditions, they have to be designed meticulously to maintain their integrity (Gonenli and Das, 2021). In order to prevent the possible damages due to these loads, the dynamic behaviors of the components should be known in advance.

* Ege University, Ege Vocational School, Department of Machine Drawing and Construction, 35100 Izmir, Turkey
Can Gonenli (can.gonenli@ege.edu.tr)

Thin plates and the many different geometries obtained from these plates are of interest to most researchers. Meyer and Scordelis (1971) presented a finite strip method to harmonic analysis of cantlever folded plate structures. Liu and Huang (1992) used the finite element-transfer matrix method to study the natural frequencies of folded plate structures. Guha Niyogi et al. (1999) employed a nine-noded Lagrangian plate element to predict the free and forced vibration response of composite folded plates. Lee et al. (2004) investigated the dynamic behavior of multiply-folded composites with the higher order plate theory. Roche et al. (2015) presented an experimental and numerical study of the folded-plate structures. Vescovini and Dozio (2016) presented an advanced approximate method for the natural frequency and buckling examination of variable stiffness thin plates. A variable-kinematic method is employed to develop a formulation in the background of a variational framework and Ritz's approach. Li et al. (2016) studied analytic vibration solutions of thin rectangular plates with or without an elastic foundation. The symplectic superposition method is employed for the solution method because many boundary value problems are generally solved by iterative methods. Robeller et al. (2017) studied the full-scale realization of a double-layered, folded plate structure. Kumar et al. (2017) studied linear and nonlinear vibration investigation of thin and thick arbitrary flat-sided quadrilateral plates with employing the finite element method. The Mindlin-Reissner plate theory is discretized with quadrilateral background cells. Bahrami et al. (2017) presented an improvement of the spectral element technique for the natural frequency analysis of thin rectangular shells exposed to impact loads. Li et al. (2018) used a rational superposition method in the symplectic space to obtain correct numerical free vibration solutions of rectangular thin cantilever plates. Based on the classical thin plate theory, Huang et al. (2018) proposed a novel series of enriched principle functions for planar and flexural displacements of square plates that can yield acceptable functions for the Ritz method using the moving least-squares. Eisenberger and Deutsch (2019) suggested novel high-efficiency numerical results that cover all the potential combinations for thin rectangular plates that solve the partial differential equations of motion. Guo et al. (2019) investigated the nonlinear vibration behavior of Z-shaped folded plates. The classical plate theory is used for the dynamic model, and the ANSYS is employed for the mode shapes. Mohammadi and Setoodeh (2019) performed free vibration analysis of functionally graded skew folded plates. The first-order shear deformation theory is employed to derive the equations of motion. Pramanik et al. (2021) investigated complex-shaped sandwich folded plate structures with and without stiffeners. Their study showed that the fixed edge of the folded plate increased the stiffness. Kumari and Saxena (2021) performed the buckling analysis on the different folded plates. The flat panel, I-section, C-section, rectangular and square-shaped folded plates are investigated. Soleimani et al. (2021) provided a structural model for the analysis of mechanical responses of Origami/Kirigami-inspired folded structures. The first-order shear deformation theory is employed and the vibrational responses of the structure are analyzed.

In this study, modal analyzes of flat plates, and folded plates obtained by bending the flat plate from the middle without changing any dimensions are investigated. Folded angles are increased from 0 degree to 90 degrees in increments of 5 degrees, and the modal analysis is repeated for each case in two different boundary conditions. The differences in the first five natural frequencies of the isotropic thin plate in all folded angles and boundary conditions are investigated. Free vibration analysis of the structure, whose dimensions are constant except the folded angle and boundary conditions, is performed and the first five natural frequencies are obtained. It can be concluded that folded plates, which are predicted to be a more stiffener structure compared to the flat plate, show different behavior under different boundary conditions. It is also seen that small geometrical changes in the structures can reveal different behaviors on the dynamic characteristics of the structure that should be known beforehand.

2. MATERIAL AND METHOD

The isotropic material type which has the same characteristics in all directions is employed to interpret the dynamic characteristics of the structural elements depending on the folded angles. Numerical details about the isotropic material are included in the results section. The thin plate is used as a structural element for flat and folded structures. The modal analyzes are performed using the ANSYS and using the element type Shell181. Shell181 is suitable for analyzing thin to moderately-thick shell structures. It is a four-node element with six degrees of freedom at each node: translations in the *x*, *y*, and *z* directions, and rotations about the *x*, *y*, and *z*-axes (Shell181 Element Description, 2021). Figure 1 shows the degrees of freedom of the finite element type.

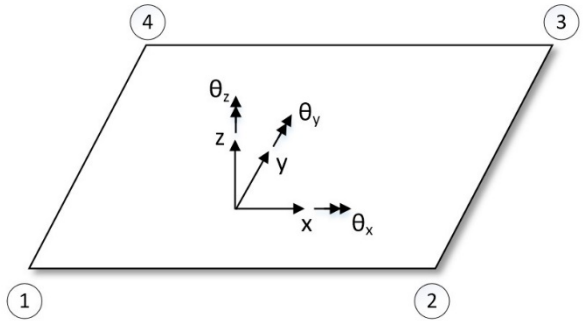

Figure 1:
The finite element type with the degrees of freedom

While examining the effect of the folded angle on the natural frequencies, the plate length is kept constant, and the plate is bent in the middle. In addition to the modal analysis of the flat plate, folded angles are started from 0 degree, and modal analysis is repeated for cantilever and two-side-fixed boundary conditions at all folded angles up to 90 degrees in increments of 5 degrees. Figure 2 shows flat and folded plate geometry.

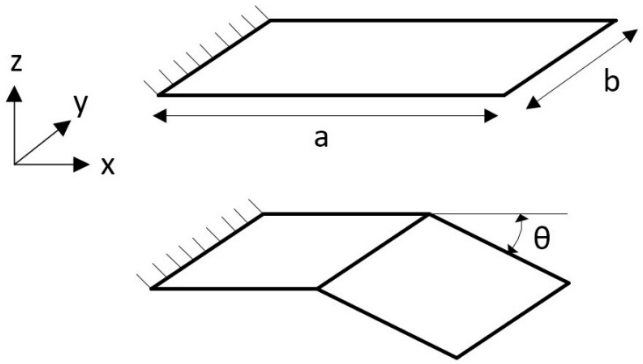

Figure 2:
Flat and folded plate structure with the representative folded angle, θ

Two different boundary conditions, which are cantilever and two-side-fixed, are applied to the structures in the modal analysis. Figure 3 shows the 45 degrees folded plates in ANSYS APDL with two different boundary conditions.

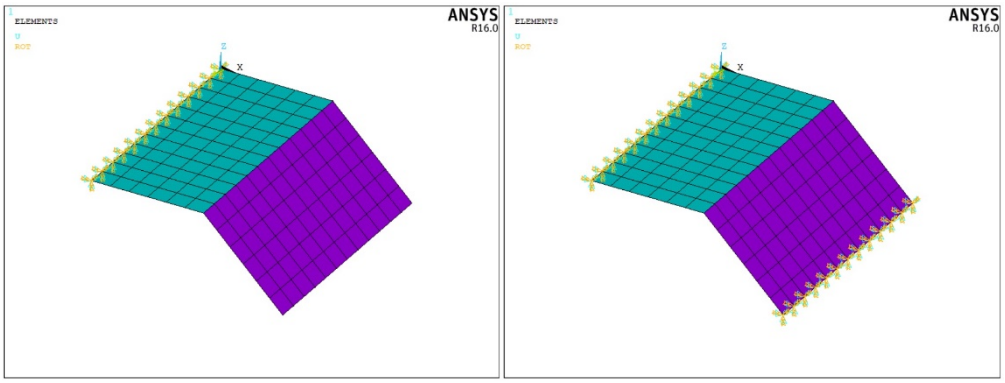

a. *b.*

Figure 3:
Two different boundary conditions on folded plate;
a. *One-side-fixed (B1)* ***b.*** *Two-side-fixed (B2)*

The natural frequencies of the structures are calculated depending on the stiffness matrix (K), and the mass matrix (M) of the structure and the equation including the generalized displacement vector (q) is presented in equation (1) (Petyt, 2015).

$$[M]\{\ddot{q}\} + [K]\{q\} = 0 \tag{1}$$

q represents the displacement vector for node j (1 to 4) and is given in equation (2).

$$q_j = \left[w_j\ \theta_{x_j}\ \theta_{y_j}\ u_j\ v_j\ \theta_{z_j}\right] \tag{2}$$

By rearranging equation (1), natural frequencies can be calculated from the eigenvalue problem given in equation (3), and here ω is the natural frequency.

$$[K] - \omega^2[M] = 0 \tag{3}$$

3. RESULTS

Isotropic material is used for flat and folded structures as mentioned in Section 2. Table-1 shows the material properties, mesh density, and boundary conditions details used in the analysis.

Table 1. Material specifications and the dimensions of the structures

Symbol	Name	Quantity
E	Modulus of Elasticity	200 GPa
ρ	Density	7800 kg/m^3
v	Poisson's Ratio	0.30
a	Length of the Plate	0.6 m
b	Width of the Plate	0.6 m

Table 1. (continued)

Symbol	Name	Quantity
h	Thickness of the Plate	10 mm
...	Mesh Density for the Structure	12 x 12
B1	Cantilever Boundary Condition	…
B2	Two-Side-Fixed Boundary Condition	…

The non-dimensional natural frequency (λ), is given in Equation (4) (Gonenli et al., 2021, Ozturk, 2011).

$$\lambda = \omega \sqrt{\frac{\rho A a^4}{EI}} \tag{4}$$

Here ω represents the natural frequency value, A represents the cross-sectional area of the structure, and I represent the moment of inertia. Table 2 and Table 3 show the first five non-dimensional natural frequency parameters for the boundary condition type 1, and 2. Dimensionless natural frequencies are obtained with both ANSYS and Solidworks for comparison. Although there are slight differences in the values due to mesh type differences, both programs show the same behavior for the first five natural frequencies within the change of the folded angle from 0 degree to 90 degrees. Also, it is seen that the values of the flat plate presented with 0 degree change in different ways as the folded angle increases.

Table 2. Comparison of the non-dimensional natural frequency parameters in ANSYS and Solidworks for the boundary condition -1

BOUNDARY CONDITION - 1										
	ANSYS					SOLID				
Angle	λ_1	λ_2	λ_3	λ_4	λ_5	λ_1	λ_2	λ_3	λ_4	λ_5
0	4.49	10.99	27.89	35.44	40.38	4.49	10.95	27.47	35.02	39.79
5	4.50	10.98	28.22	40.08	40.14	4.50	10.94	27.78	39.50	39.76
10	4.52	10.96	28.13	39.24	44.99	4.52	10.92	27.68	38.69	44.54
15	4.54	10.93	27.70	37.98	46.93	4.54	10.89	27.28	37.47	46.43
20	4.57	10.89	27.09	36.46	47.75	4.57	10.85	26.69	36.00	47.22
25	4.61	10.84	26.34	34.83	48.15	4.60	10.81	25.98	34.42	47.61
30	4.65	10.79	25.51	33.22	48.38	4.65	10.76	25.18	32.86	47.83
35	4.70	10.74	24.63	31.70	48.51	4.70	10.70	24.33	31.38	47.97

Table 2. (continued)

BOUNDARY CONDITION - 1										
	ANSYS					SOLID				
Angle	λ_1	λ_2	λ_3	λ_4	λ_5	λ_1	λ_2	λ_3	λ_4	λ_5
40	4.76	10.68	23.72	30.31	48.60	4.76	10.65	23.46	30.03	48.06
45	4.83	10.63	22.83	29.07	48.66	4.83	10.60	22.59	28.82	48.13
50	4.91	10.59	21.95	27.98	48.70	4.91	10.55	21.75	27.76	48.18
55	5.00	10.56	21.11	27.03	48.73	5.00	10.52	20.94	26.84	48.23
60	5.10	10.54	20.31	26.21	48.75	5.11	10.50	20.17	26.05	48.26
65	5.22	10.53	19.56	25.50	48.77	5.22	10.50	19.45	25.37	48.29
70	5.35	10.55	18.87	24.90	48.78	5.35	10.52	18.77	24.80	48.32
75	5.49	10.59	18.22	24.40	48.79	5.49	10.56	18.15	24.32	48.34
80	5.65	10.66	17.62	23.98	48.80	5.65	10.63	17.58	23.92	48.37
85	5.82	10.75	17.07	23.63	48.80	5.83	10.72	17.05	23.60	48.40
90	6.02	10.88	16.56	23.35	48.81	6.02	10.85	16.57	23.35	48.43

Table 3. Comparison of the non-dimensional natural frequency parameters in ANSYS and Solidworks for the boundary condition -2

BOUNDARY CONDITION - 2										
	ANSYS					SOLID				
Angle	λ_1	λ_2	λ_3	λ_4	λ_5	λ_1	λ_2	λ_3	λ_4	λ_5
0	29.22	34.52	56.62	83.50	90.76	28.80	34.27	56.42	79.38	87.19
5	45.87	49.02	69.78	83.50	90.75	45.33	48.67	69.57	79.36	87.17
10	71.81	73.51	83.50	90.73	94.15	70.50	72.58	79.36	87.18	93.56
15	83.50	90.72	91.83	93.53	114.26	79.35	87.16	88.94	91.33	112.72
20	83.50	90.71	104.18	106.53	116.14	79.34	87.15	99.58	102.85	113.64
25	83.49	90.71	111.24	114.27	116.13	79.33	87.14	105.42	109.43	113.63
30	83.49	90.70	115.38	116.12	118.90	79.33	87.14	108.79	113.31	113.63
35	83.49	90.70	116.11	117.94	121.81	79.32	87.13	110.90	113.62	115.74

Table 3. (continued)

BOUNDARY CONDITION - 2										
	ANSYS					SOLID				
Angle	λ_1	λ_2	λ_3	λ_4	λ_5	λ_1	λ_2	λ_3	λ_4	λ_5
40	83.48	90.69	116.10	119.62	123.73	79.31	87.13	112.35	113.63	117.42
45	83.48	90.68	116.09	120.77	125.05	79.32	87.14	113.40	113.63	118.62
50	83.47	90.68	116.08	121.60	126.00	79.31	87.14	113.64	114.21	119.54
55	83.46	90.67	116.06	122.21	126.71	79.30	87.13	113.65	114.88	120.28
60	83.46	90.66	116.05	122.67	127.24	79.28	87.13	113.66	115.45	120.92
65	83.45	90.65	116.03	123.03	127.66	79.28	87.14	113.69	115.96	121.48
70	83.44	90.63	116.01	123.32	127.99	79.27	87.14	113.71	116.42	121.97
75	83.42	90.62	115.99	123.55	128.26	79.26	87.14	113.72	116.86	122.42
80	83.41	90.60	115.96	123.73	128.48	79.25	87.14	113.76	117.30	122.90
85	83.39	90.58	115.93	123.89	128.66	79.23	87.14	113.77	117.68	123.29
90	83.37	90.55	115.89	124.02	128.81	79.21	87.14	113.79	118.04	123.65

Figure 4 shows the first non-dimensional natural frequency parameter changes for B1 and B2 depending on the folded angles varying between 0 and 90 degrees. While a steady increase is observed in B1 as the folded angle increased, it is seen that the folded angle had no effect on the first natural frequency from the 15-degree folded angle in B2.

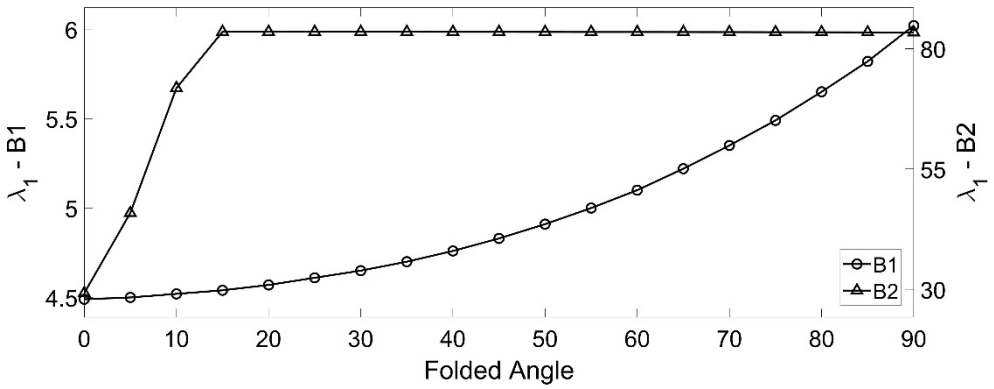

Figure 4:
Folded angle – λ curves for the first non-dimensional natural frequency parameters

In the mode shapes given in Figures 5, 7, 9, 11, and 13, the figures indicated with the letter a are for the B1 boundary condition, and the figures with the letter b are for the B2 boundary condition. In Figure 5-a1, the first mode shape for all folded angles in the B1 boundary condition is given, and in Figure 5-b, mode shapes are given with the folded angle information where the

mode shape changes. When Figure 4 and Figure 5 are examined together, it is concluded that the drastic behavior changes in the folded angle - λ curve change the mode shape.

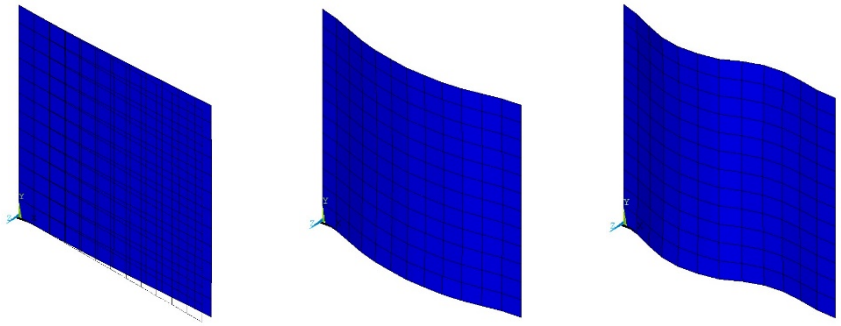

a1. *b1.* *b2.*

Figure 5:
First mode shapes;
a1. *Mode shape of B1 in 0 degree folded angle* ***b1.*** *Mode shape of B2 in 10 degree folded angle* ***b2.*** *Mode shape of B2 in 15 degree folded angle*

In Figure 6, it is seen that the behavior of the second non-dimensional natural frequency parameter for B2 does not change, from beginning a folded angle of 15 degrees. For B1, depending on the folded angle, a decrease is observed in the non-dimensional natural frequency parameters up to a 65-degree folded angle, and then an increasing trend started.

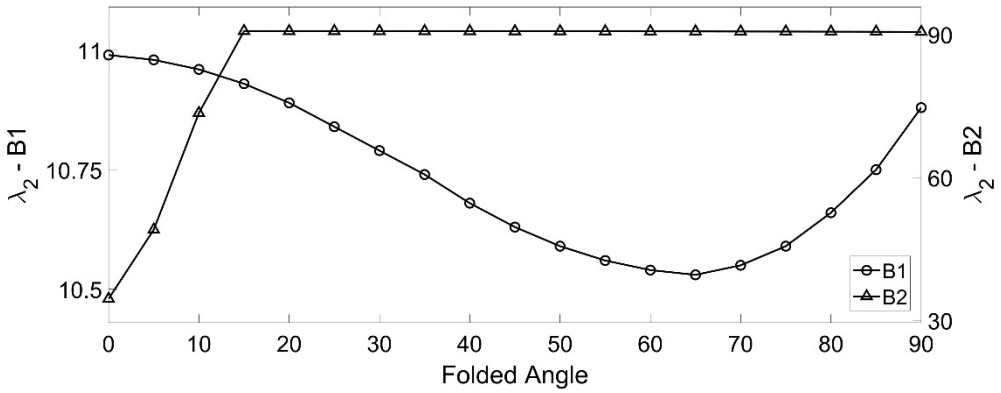

Figure 6:
Folded angle – λ curves for the second non-dimensional natural frequency parameters

Depending on the second natural frequencies, a single mode shape is observed in B1 and is given in Figure 7-a1. In Figure 7-b, the folded angle in which the mode shape changes and the two different mode shapes that occur are given for B2.

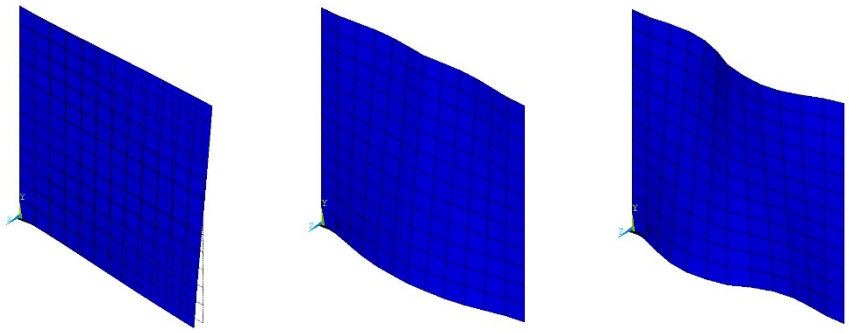

a1. *b1.* *b2.*

Figure 7:
Second mode shapes;
a1. *Mode shape of B1 in 0 degree folded angle* ***b1.*** *Mode shape of B2 in 10 degree folded angle* ***b2.*** *Mode shape of B2 in 15 degree folded angle*

In Figure 8, the variation of λ_3 values for B1 and B2 is given. In B1, it is seen that the non-dimensional natural frequency parameter increases for the small folded angles compared to the flat plate, then decreases with a behavior close to linear behavior. In B2, the change of λ_3 turned to horizontal at 30 degrees folded angle.

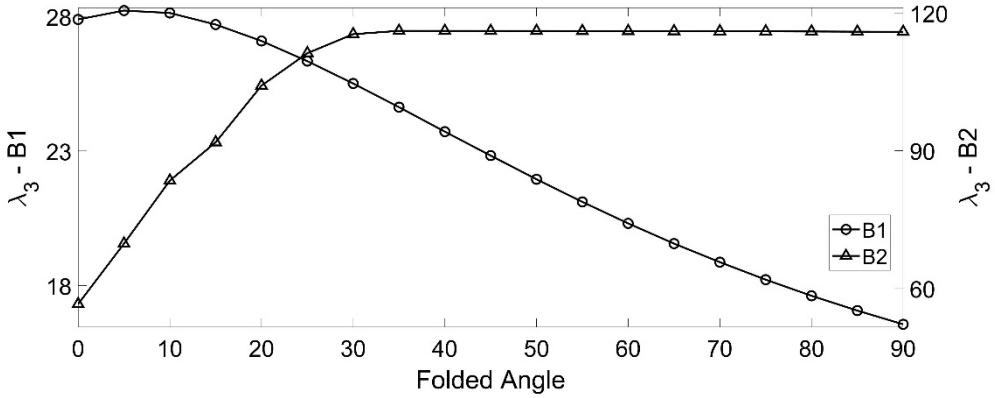

Figure 8:
Folded angle – λ curves for the third non-dimensional natural frequency parameters

A single mode shape is observed at all folded angles for B1, and is given in Figure 9-a1. For B2, 4 different mode shapes are observed.

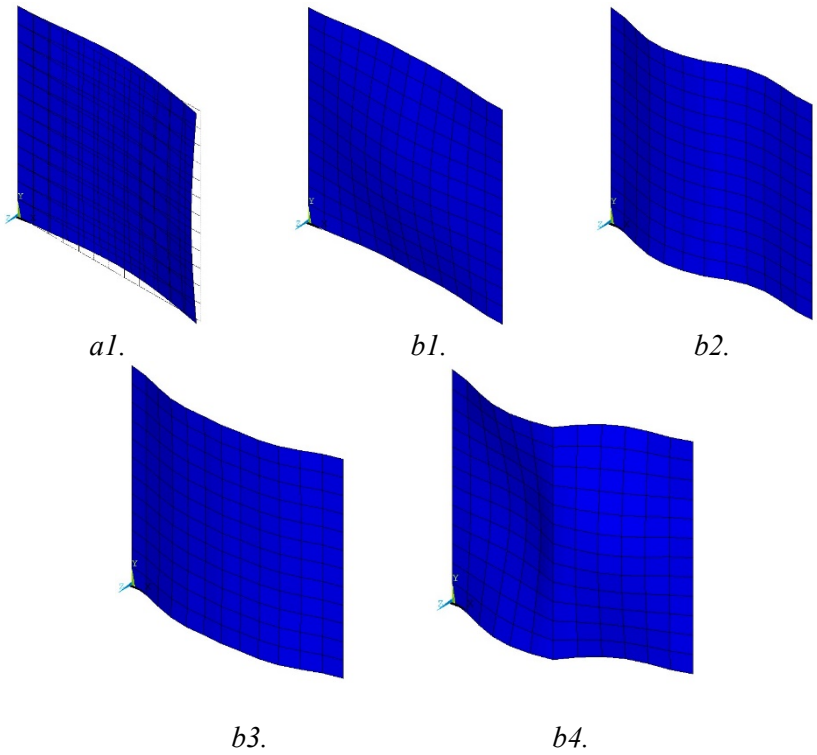

Figure 9:
Third mode shapes;
a1. *Mode shape of B1 in 0 degree folded angle* ***b1.*** *Mode shape of B2 in 5 degree folded angle* ***b2.*** *Mode shape of B2 in 10 degree folded angle* ***b3.*** *Mode shape of B2 in 15 degree folded angle* ***b4.*** *Mode shape of B2 in 35 degree folded angle*

Figure 10 shows the λ_4 changes. For the folded angle of 5 degrees in B1, an increase is observed compared to the flat plate, followed by a continuous decrease. In B2, the folded angle – λ_4 curve varies up to a 25 degree folded angle.

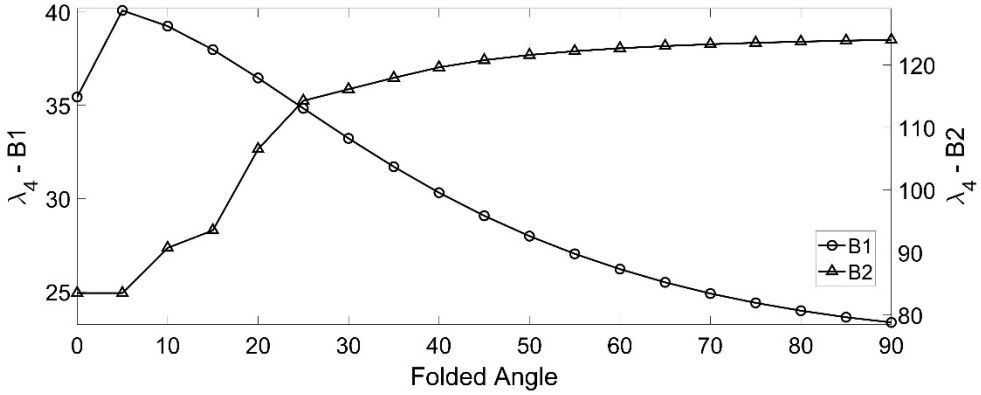

Figure 10:
Folded angle – λ curves for the fourth non-dimensional natural frequency parameters

Figure 11 presents different mode shapes for B1 and B2. While 2 different mode shapes occur for B1, 5 different modes occur for B2.

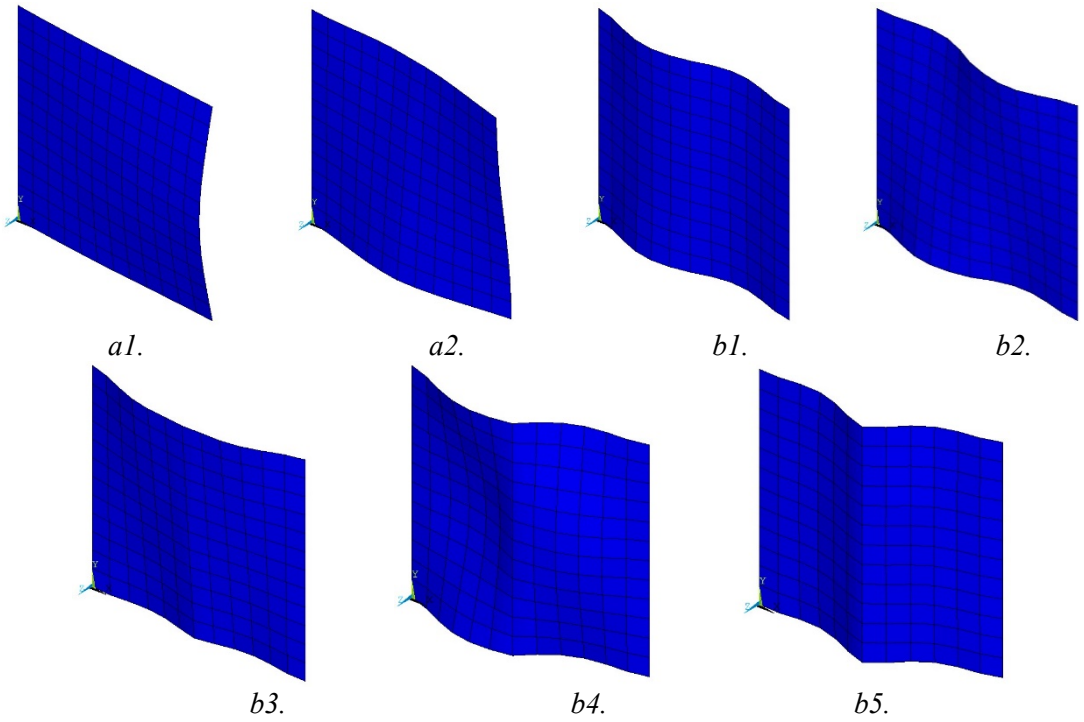

Figure 11:
Fourth mode shapes;
a1. *Mode shape of B1 in 0 degree folded angle* ***a2.*** *Mode shape of B1 in 5 degree folded angle* ***b1.*** *Mode shape of B2 in 5 degree folded angle* ***b2.*** *Mode shape of B2 in 10 degree folded angle* ***b3.*** *Mode shape of B2 in 15 degree folded angle* ***b4.*** *Mode shape of B2 in 30 degree folded angle* ***b5.*** *Mode shape of B2 in 35 degree folded angle*

Figure 12 shows B1 and B2'nin non-dimensional natural frequency parameters for λ_5. The folded angle of 5 degrees causes a decrease in the natural frequency compared to the flat plate for B1. Then an increase is seen with the folded angle increasing. The variation in the natural frequency decreases with the folded angle of 45 degrees. In B1, the changing trend is similar to the behavior of B2 in λ_4. With the 30 degrees folded angle, the folded angle – λ_4 curve becomes more stable.

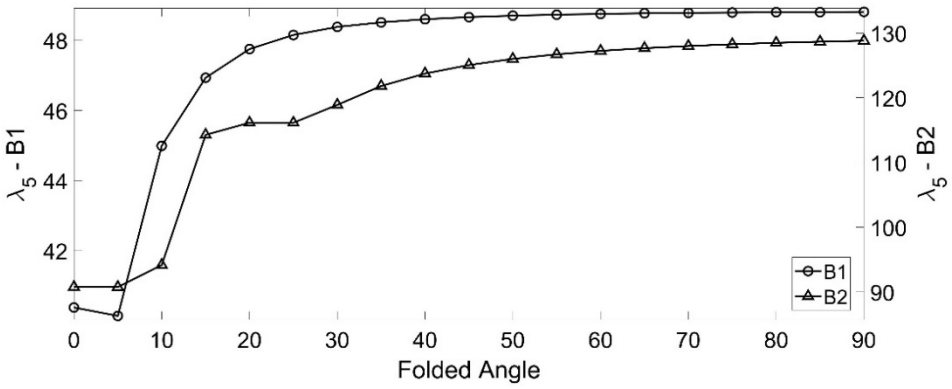

Figure 12:
Folded angle – λ curves for the fifth non-dimensional natural frequency parameters

The mode shapes of the fifth natural frequency are given in Figure 13. While 2 different modes are observed for B1, 4 different modes are observed for B2.

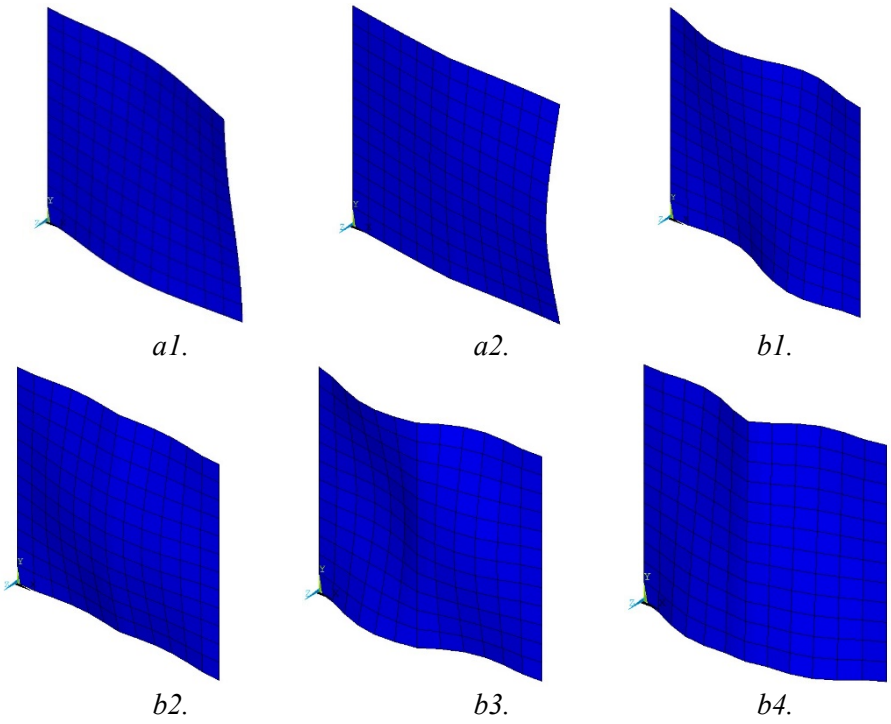

Figure 13:
Fifth mode shapes;
a1. *Mode shape of B1 in 0 degree folded angle* ***a2.*** *Mode shape of B1 in 5 degree folded angle* ***b1.*** *Mode shape of B2 in 5 degree folded angle* ***b2.*** *Mode shape of B2 in 10 degree folded angle* ***b3.*** *Mode shape of B2 in 20 degree folded angle* ***b4.*** *Mode shape of B2 in 30 degree folded angle*

The fact that the behavior is different for each natural frequency in the folded angle - λ curves with the folded angle change is of great importance to define the characteristics of the structure before the design. Rapid changes, especially at low folded angles, are the determining factors according to the properties desired to be obtained from the structure. The reason for the sudden changes in the folded angle – λ curves is that the mode shape of the relevant natural frequency of the structure changes depending on the changing geometry.

4. CONCLUSIONS

Within the scope of the study, flat and folded plates at folded angles ranging from 0 degree to 90 degrees are investigated for two different boundary conditions. While the first of the boundary condition is applied on a single edge, the second one is applied on two opposite straight edges. Both of the boundary conditions are applied on the straight edges of the structures that do not contain the folded parts. While the first boundary condition provides more free movement, the second boundary condition provides a more restricted movement to the structure. ANSYS is employed for modal analysis, and the first five natural frequencies are presented as a non-dimensional frequency parameter. According to the results:

- It has been determined that when the folded plates, which are part of the engineering structures, are exposed to different dynamic loads, their dynamic behavior can change at critical folded angles.
- As the folded angle increases, each of the natural frequencies of the structures increases or decreases in different ways.
- The increase in folded angle loses its effect on the dynamic characteristics as the angle approaches 90 degrees in the two-side-fixed boundary condition. The dynamic characteristic change due to the folded angle is more variable in the one-side-fixed boundary condition.
- The λ_2, λ_3, and λ_4 parameters are higher when the structure is flat than when the structure has a 90 degree folded angle, in the B1 boundary condition. This situation can be interpreted as a negative effect in cases where high dynamic characteristic values are desired. All five natural frequency parameters of the structure, which has a 90 degree folded angle, are higher than when the structure is flat, in the B2 boundary condition.
- The increase in folded angle affects the variation in the natural frequencies of the structure much less at higher folded angle values than the small folded angle values for two-side-fixed boundary conditions.
- Increasing at folded angle values in cantilever boundary conditions cause both a decrease and an increase in λ_2, λ_3, and λ_4.
- Sudden changes in folded angle – λ curves occur due to mode shape changes with the geometry changing.
- Compared to the flat plate, it is seen that the folded plates are unpredictable in terms of natural frequencies when one side is fixed. When the two opposite sides of the structure are fixed, the natural frequency values of the structure due to the increase of the folded angle do not show any decrease.

CONFLICT OF INTEREST

The author confirms that there is no known conflict of interest or common interest with any institution/organization or person.

AUTHOR CONTRIBUTION

Can GONENLI has the full responsibility of the paper about determining the concept of the research, data collection, data analysis and interpretation of the results, preparation of the manuscript and critical analysis of the intellectual content with the final approval.

REFERENCES

1. Bahrami, S., Shirmohammadi, F. and Saadatpour, M.M. (2017) Vibration analysis of thin shallow shells using spectral element method. *Applied Mathematical Modelling*, 44, 470–480. doi: 10.1016/j.apm.2017.02.001

2. Eisenberger, M. and Deutsch, A. (2019) Solution of thin rectangular plate vibrations for all combinations of boundary conditions. *Journal of Sound and Vibration*, 452, 1–12. doi:10.1016/j.jsv.2019.03.024

3. Gonenli, C. and Das, O. (2021) Effect of crack location on buckling and dynamic stability in plate frame structures, *Journal of the Brazilian Society of Mechanical Sciences and Engineering*, 43(6), 311. doi:10.1007/s40430-021-03032-2

4. Gonenli, C., Ozturk, H. and Das, O. (2021) Effect of crack on free vibration of a pre-stressed curved plate. *Proceedings of the Institution of Mechanical Engineers, Part C: Journal of Mechanical Engineering Science*, 095440622199486. doi:10.1177/0954406221994869

5. Guha Niyogi, A., Laha, M.K. and Sinha, P.K. (1999) Finite element vibration analysis of

laminated composite folded plate structures. *Shock and Vibration*, 6(5-6), 273-283. doi: 10.1155/1999/354234

6. Guo, X., Zhang, Y., Zhang, W. and Sun, L. (2019) Theoretical and experimental investigation on the nonlinear vibration behavior of Z-shaped folded plates with inner resonance. *Engineering Structures*, 182, 123-140. doi:10.1016/j.engstruct.2018.12.066

7. Huang, C.S., Lee, M.C. and Chang, M.J. (2018) Vibration and Buckling Analysis of Internally Cracked Square Plates by the MLS-Ritz Approach. *International Journal of Structural Stability and Dynamics*, 18(09), 1850105. doi:10.1142/S0219455418501055

8. Kumar, A., Singha, M.K. and Tiwari, V. (2017) Nonlinear bending and vibration analyses of quadrilateral composite plates. *Thin-Walled Structures*, 113, 170–180. doi:10.1016/j.tws.2017.01.011

9. Kumari, E. and Saxena, D. (2021) Buckling analysis of folded structures. *Materials Today: Proceedings*, 43, 1421-1430. doi:10.1016/j.matpr.2020.09.179

10. Lee, S.Y., Wooh, S.C. and Yhim, S.S. (2004) Dynamic behavior of folded composite plates analyzed by the third order plate theory. *International Journal of Solids and Structures*, 41(7), 1879-1892. doi:10.1016/j.ijsolstr.2003.11.026

11. Li, R., Wang, B., Li, G. and Tian, B. (2016) Hamiltonian system-based analytic modeling of the free rectangular thin plates' free vibration. *Applied Mathematical Modelling*, 40(2), 984–992. doi:10.1016/j.apm.2015.06.019

12. Li, R., Wang, P., Yang, Z., Yang, J. and Tong, L. (2018) On new analytic free vibration solutions of rectangular thin cantilever plates in the symplectic space. *Applied Mathematical Modelling*, 53, 310–318. doi:10.1016/j.apm.2017.09.011

13. Liu, W.H. and Huang, C.C. (1992). Vibration analysis of folded plates. *Journal of Sound and Vibration*, 157(1), 123-137. doi:10.1016/0022-460X(92)90570-N

14. Meyer, C. and Scordelis, A.C. (1971). Analysis of curved folded plate structures. *Journal of the Structural Division*, 97(10). doi:10.1061/JSDEAG.0003020

15. Mohammadi, H. and Setoodeh, A.R. (2019) FSDT-Based isogeometric analysis for free vibration behavior of functionally graded skew folded plates. *Iranian Journal of Science and Technology, Transactions of Mechanical Engineering*, 44, 841-863. doi:10.1007/s40997-019-00320-0

16. Ozturk, H. (2011) In-plane free vibration of a pre-stressed curved beam obtained from a large deflected cantilever beam. *Finite Elements in Analysis and Design*, 47(3), 229–236. doi:10.1016/j.finel.2010.10.003

17. Petyt, M. (2015) *Introduction to finite element vibration analysis*, Cambridge University Press, UK.

18. Pramanik, S., Das, S. and Niyogi, A.G. (2021) Free vibration and buckling analysis of stiffened sandwich plates with repeated fold. *J. Inst. Eng. India Ser. C*, 102(1), 87-98. doi:10.1007/s40032-020-00627-x

19. Robeller, C., Gamerro, J. and Weinand, Y. (2017) A double-layered timber folded plate structure. *Journal of the Association for Shell and Spatial Structures*, 58(4), 295-314. doi:10.20898/j.iass.2017.194.864

20. Roche, S., Mattoni, G. and Weinand, Y. (2015) Rotational stiffness at ridges of timber folded-plate structures. *International Journal of Space Structures*, 30(2), 153-167. doi:10.1260/0266-3511.30.2.153

21. Shell181 Element Description (2021). 4-node Structural Shell. Url: https://www.mm.bme.hu/~gyebro/files/ans_help_v182/ans_elem/Hlp_E_SHELL181.html (Access Date: 10.10.2021)

22. Soleimani, H., Goudarzi, T. and Aghdam, M.M. (2021) Advanced structural modeling of a fold in Origami/Kirigami inspired structures. *Thin-Walled Structures*, 161, 107406. doi:10.1016/j.tws.2020.107406

23. Vescovini, R. and Dozio, L.A. (2016) Variable-kinematic model for variable stiffness plates:

vibration and buckling analysis, *Composite Structures*, 142. doi:15–26. 10.1016/j.compstruct.2016.01.068